Article

Aqueous Inorganic Inks for Low-Temperature Fabrication of ZnO TFTs

Stephen T. Meyers, Jeremy T. Anderson, Celia M. Hung,
John Thompson, John F. Wager, and Douglas A. Keszler

J. Am. Chem. Soc., **2008**, 130 (51), 17603-17609 • DOI: 10.1021/ja808243k • Publication Date (Web): 03 December 2008

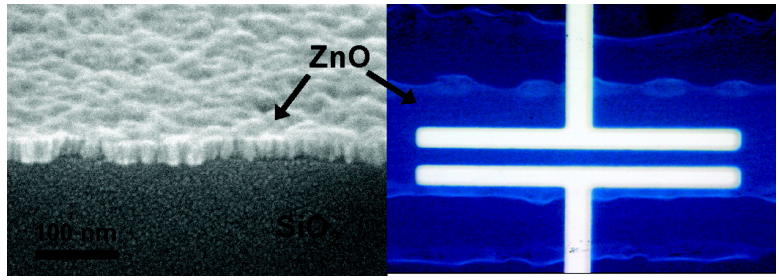

More About This Article

Additional resources and features associated with this article are available within the HTML version:

- Supporting Information
- Access to high resolution figures
- Links to articles and content related to this article
- Copyright permission to reproduce figures and/or text from this article

View the Full Text HTML

J|A|C|S
ARTICLES

Published on Web 12/03/2008

Aqueous Inorganic Inks for Low-Temperature Fabrication of ZnO TFTs

Stephen T. Meyers,[†] Jeremy T. Anderson,[†] Celia M. Hung,[‡] John Thompson,[§] John F. Wager,[‡] and Douglas A. Keszler*,[†]

Department of Chemistry, Oregon State University, 153 Gilbert Hall, Corvallis, Oregon 97331-4003, School of Electrical Engineering and Computer Science, Oregon State University, Corvallis, Oregon 97331-5501, and Hewlett-Packard Company, 1000 NE Circle Boulevard, Corvallis, Oregon 97330

Received October 20, 2008; E-mail: douglas.keszler@oregonstate.edu

Abstract: A simple, low-cost, and nontoxic aqueous ink chemistry is described for digital printing of ZnO films. Selective design through controlled precipitation, purification, and dissolution affords an aqueous $Zn(OH)_x(NH_3)_y^{(2-x)+}$ solution that is stable in storage, yet promptly decomposes at temperatures below 150 °C to form wurtzite ZnO. Dense, high-quality, polycrystalline ZnO films are deposited by ink-jet printing and spin-coating, and film structure is elucidated via X-ray diffraction and electron microscopy. Semiconductor film functionality and quality are examined through integration in bottom-gate thin-film transistors. Enhancement-mode TFTs with ink-jet printed ZnO channels annealed at 300 °C are found to exhibit strong field effect and excellent current saturation in tandem with incremental mobilities from 4−6 $cm^2\ V^{-1}\ s^{-1}$. Spin-coated ZnO semiconductors processed at 150 °C are integrated with solution-deposited aluminum oxide phosphate dielectrics in functional transistors, demonstrating both high performance, i.e., mobilities up to 1.8 $cm^2\ V^{-1}\ s^{-1}$, and the potential for low-temperature solution processing of all-oxide electronics.

Introduction

A convergence of electronic and chemical properties in ZnO make it one of the more widely used metal oxides with applications ranging from catalysis to cosmetics, fungicides to phosphors, and pigments to polymer additives. In recent years, the material has garnered additional attention as a channel material for high-performance transparent thin-film transistors (TFTs). Part of a large class of semiconducting oxides,[1,2] the facile thin-film processing of ZnO has enabled physical vapor deposition (PVD) fabrication of ZnO TFTs with a wide variety of gate dielectrics, even extending to flexible substrates.[3−5] Since the beginning of this ZnO TFT renaissance (the first ZnO TFT was proposed in 1968),[6] a coincident effort has been made to develop solution-based methods for large-area, low-cost, and low-temperature printing of ZnO films for macroelectronic applications. These efforts, however, have been hampered by a lack of solution precursors appropriate for a high-speed, low-temperature printing process. The defect and solution chemistries of ZnO, vital to electrical performance and film quality, have been too often ignored in favor of the ready application of conventional metal−organic preparative routes common to ceramic synthesis. In the present contribution, we demonstrate a simple aqueous precursor specifically designed to take advantage of the unique solution chemistry of Zn. This nontoxic, aqueous chemistry generates high-quality ZnO films at low temperatures, allowing ink-jet printing of high-performance ZnO-channel TFTs at 150 °C.

Such chemistries have not previously been demonstrated, despite the voluminous literature concerning solution-processed ZnO thin films. Instead, the condensation and crystallization of ZnO from aqueous solutions has been utilized in more circuitous routes to nanocrystalline films. Reports of chemical bath deposition (CBD) are prevalent, though this process is incompatible with high-speed printing. Moreover, although careful attention to CBD thermodynamics permits the deposition of ZnO films at temperatures below 100 °C,[7] TFTs fabricated by this method have until recently[8] performed very poorly in the absence of high-temperature annealing.[9,10] The deposition and sintering of nanoparticle suspensions following a procedure of decoupled growth and deposition is also quite common.[11] Low-temperature sintering, however, typically results in porous nanoparticle agglomerates with a preponderance of interface

[†] Department of Chemistry, Oregon State University.
[‡] School of Electrical Engineering and Computer Science, Oregon State University.
[§] Hewlett-Packard Company.

(1) Hosono, H. *J. Non-Cryst. Solids* **2006**, *352*, 851.
(2) Chiang, H. Q.; Wager, J. F.; Hoffman, R. L.; Jeong, J.; Keszler, D. A. *Appl. Phys. Lett.* **2005**, *86*, 013503.
(3) Hoffman, R. L.; Norris, B. J.; Wager, J. F. *Appl. Phys. Lett.* **2003**, *82*, 733.
(4) Carcia, P. F.; McLean, R. S.; Reilly, M. H. *Appl. Phys. Lett.* **2006**, *88*, 123509.
(5) Carcia, P. F.; McLean, R. S.; Reilly, M. H. *J. SID.* **2005**, *13*, 547.
(6) Boesoen, G. F.; Jacobs, J. E. *Proc. IEEE* **1968**, *56*, 2094.
(7) Govender, K.; Boyle, D. S.; Kenway, P. B.; O'Brien, P. *J. Mater. Chem.* **2004**, *14*, 2575.
(8) Li, C.; Li, Y.; Wu, Y.; Ong, B. S.; Loutfy, R. O. *J. Appl. Phys.* **2007**, *102*, 076101.
(9) Cheng, H.; Chen, C.; Lee, C. *Thin Solid Films.* **2006**, *498*, 142.
(10) Redinger, D.; Subramanian, V. *IEEE Trans. Electron Devices* **2007**, *54*, 1301.
(11) Volkman, S. K.; Mattis, B. A.; Molesa, S. E.; Lee, J. B.; de la Fuente Vombeck, A.; Bakhishev, T.; Subramanian, V. *IEEE Int. Electron Device Meeting Tech. Dig.* **2004**, 769.

states that not only limit carrier mobility, but also adversely affect TFT subthreshold slope, off current, and switching voltage. Hybrid approaches using combinations of aligned nanoparticles, sol−gel,[12] and CBD[13,14] have overcome some of these density issues at the expense of process flexibility; ZnO TFTs processed at 270 °C, for example, have exhibited saturation mobilities up to 1.3 $cm^2\ V^{-1}\ s^{-1}$.[15] Yet, to date, all purely chemical precursors compatible with high-speed direct printing require high-temperature (≥500 °C) processing,[16−19] reflective of the high activation and diffusion energies attendant to metal−organic sol−gel[20] and oxidative/hydrolytic[21,22] decomposition reactions.

In contrast to these kinetically limited, complex, and energy-intensive processes, we have advanced simple cation hydration chemistries in designing environmentally benign and highly reactive aqueous precursors for deposition of very high-quality oxide films.[23,24] Here, purified ammine−hydroxo zinc solutions tap the rapid, low-energy kinetics of metal−ammine dissociation and hydroxide condensation/dehydration reactions to afford crystallization of ZnO near room temperature. This minimalist approach to precursor synthesis provides superior film quality, while at the same time enabling high-throughput digital printing via ink-jet deposition. Building on our previous solution deposition of oxide dielectrics, we further demonstrate the potential for all-oxide printed electronics through fabrication of the first high-performance TFTs containing both solution-processed oxide dielectric and semiconductor layers. A ZnO semiconductor layer annealed at 150 °C is combined with a solution-processed aluminum oxide phosphate (AlPO) dielectric to yield a device exhibiting a field-effect mobility near 2 $cm^2\ V^{-1}\ s^{-1}$.

Experimental Methods

Precursor Synthesis and Analysis. Zn solutions were prepared by dissolving $Zn(NO_3)_2 \cdot 6H_2O$ (Alfa Aesar, 99.998%) in distilled H_2O to a total concentration of 0.5 M Zn. Ten milliliters of 2.5 M NaOH (Mallinckrodt, ACS) was added dropwise to 15 mL of this solution over the course of 5 min while stirring vigorously. The resulting hydroxide slurry was centrifuged and the supernatant removed. The hydrated precipitate was then suspended in 20 mL of H_2O and agitated for 2 min, followed by centrifugation and supernatant removal. Rinse and separation steps were repeated four additional times to minimize Na^+ and NO_3^- concentrations. Following final centrifugation, the supernatant was decanted a final time and the hydrated precipitate dissolved in 50 mL of 6.6 M NH_3(aq) (Alfa Aesar, 99.99%) to form a stock precursor. The final Zn concentration in the stock precursor solution was 0.14 M. Millipore H_2O with a minimum resistivity of 18 MΩ was used for all dilutions and rinses. Na and impurity concentration data were generated with a Perkin-Elmer 3000DV inductively coupled plasma optical emission spectrometer (ICP-OES). Reported data represent the mean of three consecutive replicate measurements using a minimum of two check standards to bracket measured concentrations. Bulk ZnO powders were produced for X-ray diffraction (XRD) measurements by placing a known volume of the precursor solution in a glass vial, evaporating the solvent, and dehydrating the resulting powder in a drying oven in air for 24 h at 50 °C. Powder XRD data were collected by using a Siemens D5000 diffractometer with Cu Kα radiation.

Film Preparation and Analysis. Thin films were deposited by spin-coating the stock precursor solution filtered through a 0.45-μm PTFE syringe filter. Substrate rotation speed and time were 3000 rpm and 30 s. The film was then immediately cured on a preheated hot plate at selected temperatures between 150 and 500 °C for 5−10 min. Inks for thermal ink-jet (TIJ) printing were prepared by dilution of the stock solution with isopropanol (Aldrich, 99.5% ACS), aqueous ammonia, and H_2O to a final concentration of 5.3 M NH_3(aq), 0.056 M Zn, and 40% (vol) isopropanol. Isopropanol is used solely to decrease solution surface tension to allow reliable jetting. Films were printed by promptly filling commercial Hewlett-Packard (HP-80) printer cartridges and printing $1 \times 15\ mm^2$ lines directly onto precleaned substrates at room temperature. Printing was followed by immediate hot-plate curing in air for 5−10 min at selected temperatures between 150 and 500 °C. Coating and curing steps were repeated as necessary to obtain the desired thickness. A final anneal at the same temperature was done either in air or in a tube furnace under 150 sccm flowing N_2(g) or Ar(g). Thin films for XRD and scanning electron microscopy (SEM) were deposited on substrates of 200-nm thick thermally grown SiO_2 on Si. All substrates were cleaned by sonication in a 5% solution of Contrad 70 for 45 min at 45 °C followed by thorough rinsing with 18-MΩ H_2O. Thin-film XRD data were collected by using a Rigaku RAPID diffractometer with Cu Kα radiation.

Device Fabrication and Characterization. Bottom-gate TFT test structures were fabricated by TIJ printing or spin coating ZnO semiconductor films of 15−40 nm thickness onto a 100-nm SiO_2 gate dielectric thermally grown on *p*-type Si substrates with 30 nm of Ta and 300 nm of Au on the back side to allow gate probing through the substrate. Aluminum oxide phosphate (AlPO) precursor solutions were prepared as previously reported.[24] Sixty-nanometer AlPO gate dielectric films were spin-coated on bare, p^{+2} Si substrates and subjected to a postdeposition anneal at 500 °C for 1 h prior to ZnO deposition. One-hundred or 200-nm thick Al source and drain contacts were then thermally evaporated via shadow mask onto ZnO films to complete device stacks. All TFTs were characterized in the dark under atmospheric conditions by using Hewlett-Packard 4156C and 4155A semiconductor parameter analyzers; device mobility and operational parameters were evaluated following the methods of Hoffman.[25]

Results and Discussion

Precursor Chemistry and Analysis. The fundamental chemical requirement for any solution printing process is the complete conversion of the precursor ink into a target oxide of the correct phase. All solvents and ligands must be eliminated under the desired processing conditions and within the thermal budget. Circuitous metal−organic routes typically sacrifice simplicity and reactivity for the sake of perceived improvements in

(12) Cheng, H.-C.; Chen, C.-F.; Tsay, C.-Y. *Appl. Phys. Lett.* **2007**, *90*, 012113.
(13) Sun, B.; Sirringhaus, H. *Nano Lett.* **2005**, *5*, 2408.
(14) Sun, B.; Sirringhaus, H. *J. Am. Chem. Soc.* **2006**, *128*, 16231.
(15) Sun, B.; Peterson, R. L.; Sirringhaus, H.; Mori, K. *J. Phys. Chem. C.* **2007**, *111*, 18831.
(16) Norris, B. J.; Anderson, J. T.; Wager, J. F.; Keszler, D. A. *J. Phys. D: Appl. Phys.* **2003**, *36*, L105.
(17) Lee, J. H.; Lin, P.; Ho, J. C.; Lee, C. C. *Electrochem. Solid-State Lett.* **2006**, *9*, G117.
(18) Lee, J. H.; Lin, P.; Ho, J. C.; Lee, C. C.; Wang, Y. W. *Jpn. J. Appl. Phys.* **2005**, *44*, 2005.
(19) Ong, B. S.; Li, C.; Li, Y.; Wu, Y.; Loutfy, R. *J. Am. Chem. Soc.* **2007**, *129*, 2750.
(20) Bhuiyan, M. S.; Paranthaman, M.; Salama, K. *Supercond. Sci. Technol.* **2006**, *19*, R1.
(21) Chang, Y.-J.; Lee, D.-H.; Herman, G. S.; Chang, C.-H. *Electrochem. Solid-State Lett.* **2007**, *10*, H135.
(22) Lee, D.-H.; Chang, Y.-J.; Herman, G. S.; Chang, C.-H. *Adv. Mater.* **2007**, *19*, 843.
(23) Anderson, J., T.; Keszler, D. A.; Meyers, S. T.; Chiang, H. Q.; Hong, D.; Presley, R. E.; Wager, J. F. *Mater. Res. Soc. Symp. Proc.* **2007**, *988E*, 0988.
(24) Meyers, S. T.; Anderson, J., T.; Hong, D.; Hung, C. M.; Wager, J. F.; Keszler, D. A. *Chem. Mater.* **2007**, *19*, 4023.
(25) Hoffman, R. L. *J. Appl. Phys.* **2004**, *95*, 5813.

rheological properties.[20] The primary result is that otherwise rapid and highly favorable reactions, i.e., the hydrolysis and subsequent hydroxo-condensation of the metal species, instead require extreme activation and diffusion energies to complete. In contrast, the simplicity and reactivity inherent to aqueous Zn chemistry render an all-inorganic hydroxo-condensation approach extremely attractive. ZnO is amphoteric in nature and the weak acidity of the Zn^{2+} ion affords a wide solubility range. The low activation energy required for $Zn(OH)_2$ dehydration and oxide crystallization is complementary to low-temperature deposition, as opposed to the much higher energies required for complete dehydration of hydroxides such as $In(OH)_3$ and $Sn(OH)_4$.[26,27] Furthermore, Zn, in common with many borderline Lewis acids, readily forms coordination complexes with ammonia in an aqueous environment. Ammonia is distinguished from other nitrogen-based ligands by its extreme volatility and labile bonding which afford low-temperature, rapid, and (equally important) low volume-loss decomposition processes. Although the solubility of Zn in aqueous ammonia is relatively high, the kinetic obstacles to oxide dissolution are such that directly dissolving large-grain ZnO powders is difficult. Nevertheless, to fully exploit the excellent low temperature thermodynamics and rapid kinetics of ammine-hydroxo zinc decomposition, nonbasic counterions must be excluded, prohibiting simple dissolution of Zn salts in aqueous ammonia. To circumvent this barrier, fresh $Zn(OH)_2$ precipitates may be purified and directly dissolved in NH_3(aq) solutions. Such processes have been used for more than 80 years as part of bulk ZnO purification and synthesis procedures.[28] The predominant form of the aqueous ammine-hydroxo zinc complex that results depends on the ammonia concentration,[29] but it may be described by the general formula $Zn(OH)_x(NH_3)_y^{(2-x)+}$. Properly purified, these solutions are largely free of nonbasic counterion contaminants, and precipitate a pure phase hydroxide upon ammonia loss, followed by dehydration and oxide crystallization at temperatures below 100 °C.

Synthetic conditions in the present study were intended to provide both a minimal impurity concentration and a low-temperature, nonhydrolytic decomposition mechanism for the inevitable residual ions. Selection of the initial soluble $Zn(NO_3)_2$ salt is important in pursuit of the second goal, as polarization of the NO_3^- charge cloud by acidic cations is known to result in reasonably low decomposition temperatures for nitrate salts of acidic metal cations.[30] A study of zinc ammine hydroxide nitrates by Bénard and co-workers[31] provides evidence that $Zn_5(OH)_8(NO_3)_2 \cdot 2NH_3$ and related compounds offer very low decomposition and ZnO crystallization temperatures, generally <150 °C, with NH_3 loss occurring well below 100 °C. These results contrast starkly with thermal-analysis studies of zinc chloride hydroxide compounds including $Zn_5(OH)_8Cl_2 \cdot H_2O$ and β-ZnOHCl by Srivastava and Secco,[32] which confirm the expectation that basic halides not only dehydrate at much higher temperatures than the pure hydroxides, but that hydrolytic or oxidative removal of the residual metal chloride may require

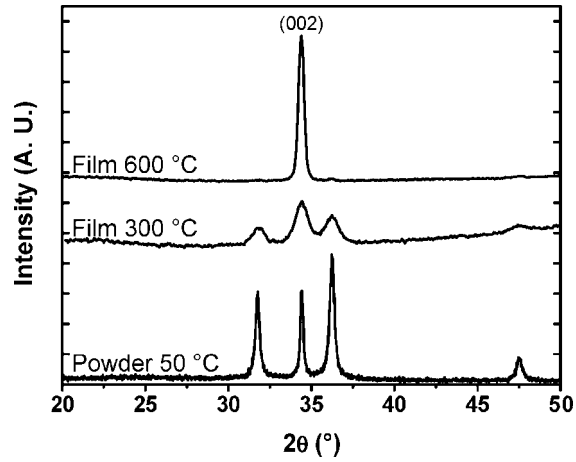

Figure 1. X-ray diffraction patterns of a wurtzite ZnO powder obtained through decomposition of a zinc−ammine precursor ink at 50 °C in air for 24 h. This randomly oriented powder is contrasted with the increasing degree of (002) orientation observed in diffraction patterns of spin-coated ZnO films deposited via 10 coating and curing cycles and annealed at the indicated temperature for 1 h.

significant heating, antithetical to the intended rapid, low-temperature reaction. Precipitation conditions were likewise modified by the slow addition of a large mole ratio of a strong base (NaOH) to promote hydroxide displacement of the nitrate anion and increase precipitate purity relative to initially favored precipitation with NH_3(aq). Extensive rinsing of the precipitate is employed to remove deleterious Na^+ contaminants. ICP-OES analysis of a standard zinc−ammine solution prepared from this precipitate after five centrifugation and rinse cycles reveals Na contamination below the 4 ppm detection limit (<0.03% relative to Zn). Dehydration of ammine-hydroxo zinc solutions prepared from these precipitates in a drying oven at 50 °C for 24 h generates a powder with the diffraction pattern seen in Figure 1, characteristic of large-domain hexagonal ZnO. TGA measurements on identical powders show a total mass loss <1.5% when heated from 50−600 at 10 °C/min, indicating substantial chemical purity following low temperature decomposition.

It is important to note that these slow bulk evaporation, dehydration, and crystallization processes are only partially analogous to the rapid, kinetically constrained printing and dehydration of hydroxide thin films. Indeed, the initial loss of ammonia under heating probably yields supersaturated $Zn(OH)_x^{(2-x)+}$ species and nucleation thermodynamics closely related to those described during CBD. However, total evaporation of the solution drives unique reactions and offers macroscopic verification of the key ink decomposition requirements for additive printing processes. A simplified precipitation, dissolution, and deposition scheme may be expressed as

$$Zn(NO_3)_2(aq) + 2NaOH(aq) \rightarrow Zn(OH)_2(s) + 2NaNO_3(aq) \quad (1)$$

$$Zn(OH)_2(s) + xNH_3(aq) \rightarrow Zn(OH)_2(NH_3)_x(aq) \rightarrow ZnO(s) + xNH_3(g) + H_2O(g) \quad (2)$$

Film Morphology and Composition. High-performance printed-semiconductor channels necessitate not only chemical and phase purity following low-temperature deposition, but also a dense, homogeneous morphology. While often overlooked, the influence of grain morphology and film density on the operational parameters of TFTs is difficult to overstate. This is apparent in ZnO devices fabricated from sintered nanoparticle arrays

(26) Giesekke, E. W.; Gutaowsky, H. S.; Kirkov, P.; Laitinen, H. A. *Inorg. Chem.* **1967**, *6*, 1294.
(27) Sato, T. *J. Therm. Anal. Calorim.* **2005**, *82*, 775.
(28) Dietrich, H. G.; Johnston, J. *J. Am. Chem. Soc.* **1927**, *49*, 1419.
(29) Danilov, V. V.; Ravdel, A. A.; Lutsik, V. P. *Zh. Obshch. Khim.* **1976**, *46*, 976.
(30) Yuvaraj, S.; Fan-Yuan, L.; Tsong-Huei, C.; Chuin-Tih, Y. *J. Phys. Chem. B.* **2003**, *107*, 1044.
(31) Bénard, P.; Auffrédic, J. P.; Louër, D. *Thermochim. Acta* **1994**, *232*, 65.
(32) Srivastava, O. K.; Secco, E. A. *Can. J. Chem.* **1966**, *45*, 579.

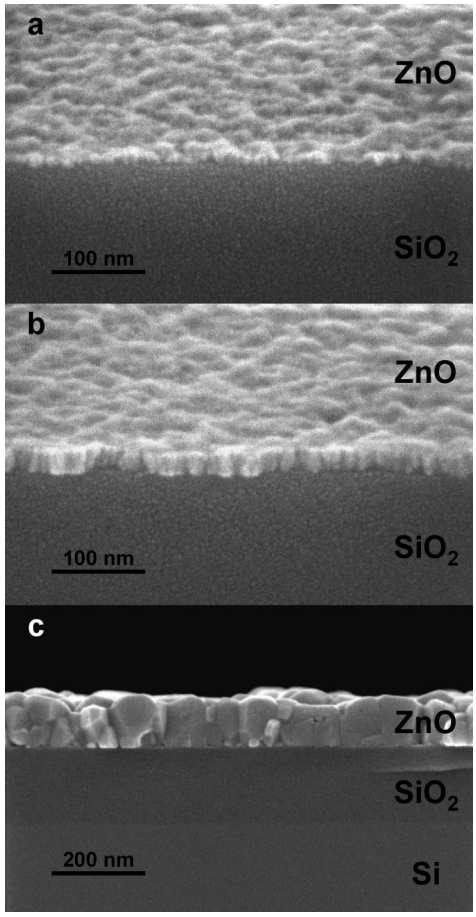

Figure 2. SEM cross section and 45° tilt images of ink-jet printed ZnO thin films annealed at (a) 150 and (b) 300 °C. (c) A spin-coated film annealed to 600 °C in air.

wherein individual nanocrystals may have high mobilities,[33,34] yet carrier modulation and mobility in the TFT channel is dominated by discrete interfaces between nominally sintered nanoparticles with high surface areas and consequent surface-stabilized shallow donors.[11] Therefore, in seeking low-temperature device performance the as-deposited morphology must be as dense as possible, given that large-scale sintering and grain growth are not energetically favorable at low temperatures. SEM images of printed and spin-coated ZnO films prepared from aqueous zinc−ammine precursors are seen in Figure 2. Printed films are considerably thinner than spin-coated films due to concentration limitations for reliable jetting and the substantial solubility of small-grain ZnO films in ammonia, which prevents successive layer-on-layer coating without an interlayer cure of at least 300 °C. However, even thin (∼15 nm) films annealed at 150 °C appear dense and continuous. Annealing to 300 °C between printing passes produces a more regular morphology, and thicker films (20 nm) with three printing passes. Repeated spin-coating cycles of higher Zn concentrations, coupled with annealing temperatures of 600 °C result in ∼200 nm films with large columnar grains. The dense, homogeneous morphology possible from this chemistry directly correlates with high performance devices and contrasts starkly with the porous nanocrystal arrays commonly encountered in literature reports.

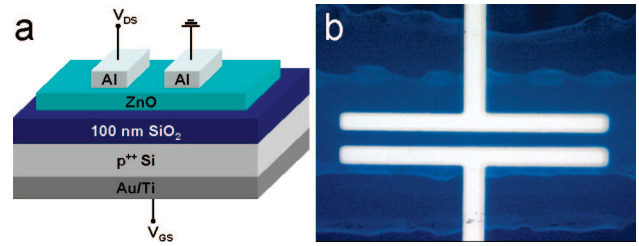

Figure 3. (a) Schematic structure of the bottom-gate TFT test structure used for both printed and spin-coated ZnO devices. For the device shown in Figure 6 the SiO_2 insulator is replaced by a 60-nm spin-coated AlPO dielectric. (b) Optical microscope image of a printed ZnO-channel TFT on SiO_2.

Table 1. Representative Performance Parameters for Solution-Processed ZnO-Channel TFTs

anneal (°C)	ambient	V_{on}	μ_{inc}(cm^2/Vs)	I_{on}/I_{off}
150	flowing N_2	12	0.4	10^6
200	flowing N_2	10	0.7	10^6
300	flowing N_2	3	4.3	$>10^6$
400	air	−1	3.3	$>10^6$
500	air	−7	6.1	$>10^6$
150[a]	air	1	1.8	10^6
300[b]	air	3	3.1	10^6

[a] Spin-coated ZnO on AlPO dielectric. [b] Spin-coated ZnO on SiO_2 dielectric.

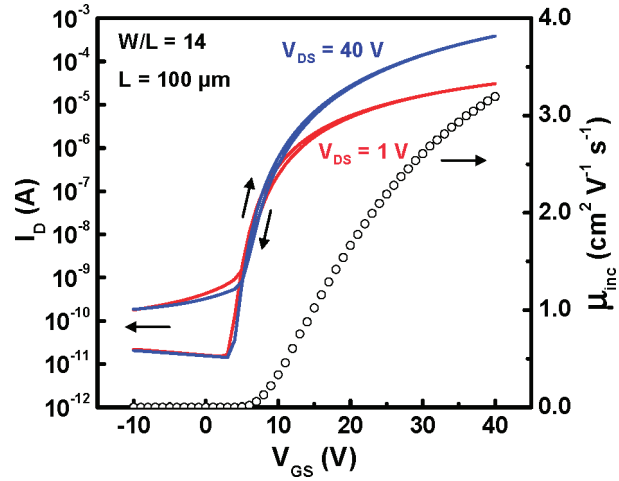

Figure 4. $\log(I_D) - V_{GS}$ transfer and $\mu_{inc} - V_{GS}$ characteristics for a TFT with a spin-coated ZnO-channel annealed at 300 °C in air. The gate dielectric for this device is 100 nm thermal SiO_2. $V_{th} = 14.5$ V.

While similar solutions have been employed in low-temperature selective ionic layer absorption and reaction (SILAR) depositions,[35] thermodynamics in these relatively slow surface-mediated reactions favor nucleation of isolated crystallites and anisotropic growth in selective orientations with discrete interfaces and corresponding morphologies. In contrast, the rapid kinetics of dehydration, condensation, and ammine decomposition reactions in the present printed and spin-coated films prevent long-range anisotropic particle growth, preserving film continuity.

All ZnO films in this study exhibit diffraction patterns consistent with the hexagonal wurtzite structure. Printed and spin-coated films cured at temperatures <300 °C were extremely thin (<20 nm), preventing extensive XRD analysis beyond simple phase identification with grazing incidence diffraction.

(33) Noh, Y.-Y.; Cheng, X.; Sirringhaus, H.; Sohn, J. I.; Welland, M.; Kang, D. J. *Appl. Phys. Lett.* **2007**, *91*, 043107.
(34) Goldberger, J.; Sirbuly, D. J.; Law, M.; Yang, P. *J. Phys. Chem. B.* **2005**, *109*, 9.
(35) Gao, X.; Li, X.; Yu, W. *Wuji Cailiao Xuebao* **2004**, *19*, 610.

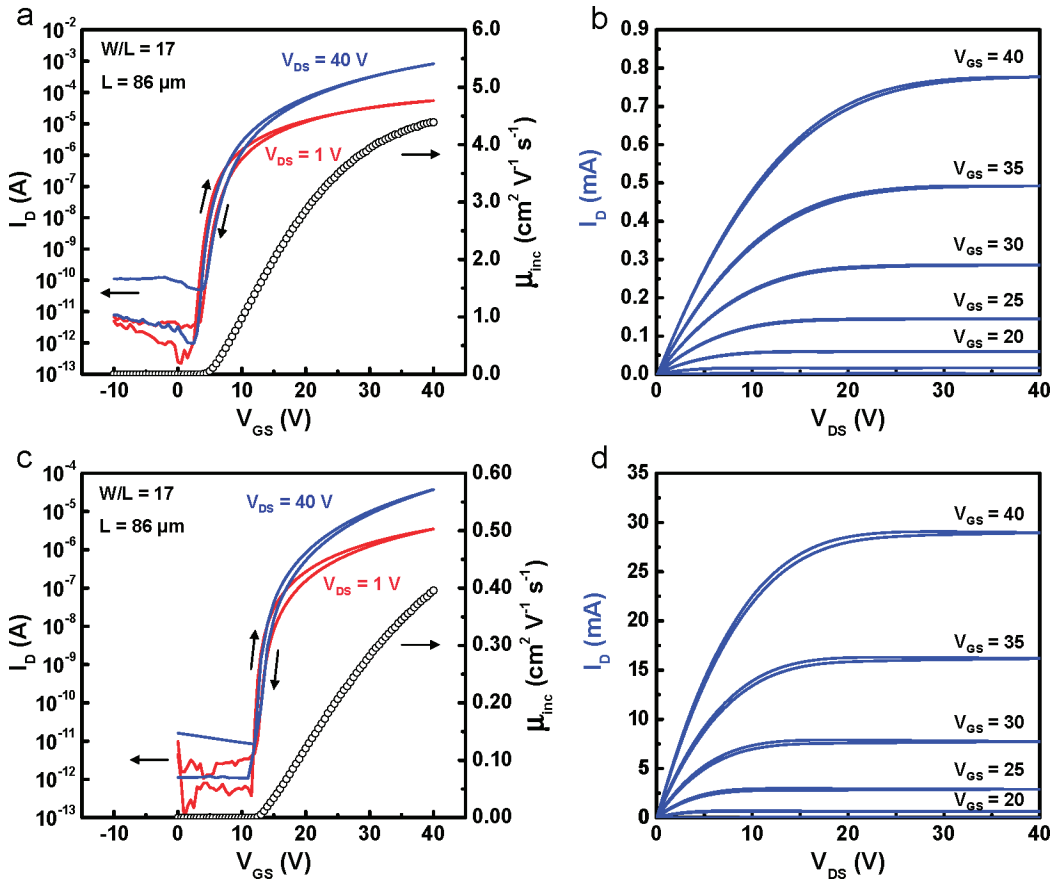

Figure 5. $\log(I_D) - V_{GS}$ transfer and $\mu_{inc} - V_{GS}$ characteristics and $I_D - V_{DS}$ output curves for ink-jet printed ZnO-channel TFTs on 100-nm thermal SiO_2 gate dielectrics.; channel annealed in flowing N_2(g) at (a) and (b) 300 °C and (c) and (d) 150 °C. V_{th} = 15 and 20 V, respectively.

Interlayer curing ≥300 °C allowed sequential coatings and thicker films. X-ray diffraction patterns obtained from sequentially spin-coated ZnO films annealed at 300 and 600 °C are documented in Figure 1. As manifest in the prominent (002) reflection observed at 34.4°, these films demonstrate a varying degree of *c*-axis orientation, increasing significantly with additional deposition cycles and elevated interlayer curing temperature. Substantial *c*-axis orientation is frequently reported following high-temperature deposition of ZnO films from both solution and vapor techniques, as grain growth tends to favor the low energy (002) surface.[36] Although not examined in the present study, the effect of this texturing on electron mobility has been reported to be significant.[19]

Electrical Characterization. Electrical analyses of ZnO films were performed by using the bottom-gate TFT structure depicted in Figure 3a. Device performance is assessed through an analysis of the turn-on voltage (V_{on}), drain current on-to-off ratio (I_{on}/I_{off}), and incremental channel mobility (μ_{inc}). Hoffman[25] and Hong et al.[37] have defined V_{on} as the gate voltage at which I_D begins to increase when plotted versus V_{GS} on a logarithmic scale. It is here employed in place of the threshold voltage (V_{th}) due to its greater precision in the context of TFT characterization. Poor turn-on (extremely negative or positive V_{on}) characteristics are unsuitable for most circuit applications. A low I_{on}/I_{off} ratio prevents the device from operating as a high dynamic range switch, the primary application for which TFTs are typically employed. Channel mobility directly relates to TFT current drive and maximum switching frequency, and represents a useful figure of merit provided the former parameters are acceptable. The incremental, or field-effect mobility quoted here is extracted in linear-regime operation at V_{DS} = 1 V. A final parameter, the subthreshold swing (*S*)—defined as the gate voltage required to change the drain current by 1 order of magnitude in the subthreshold region of the transfer curve—provides a measure of how effective applied gate voltage is in turning the channel on and off.[38] It is imperative that all of these parameters are optimized for a truly useful device; a tabulation of solution-deposited ZnO-channel TFT performance parameters representative of more than 250 devices may be found in Table 1.

TFTs fabricated with spin-coated ZnO channels annealed at 300 °C in air on thermally grown SiO_2 dielectrics display promising operation, as evident from the transfer curves plotted in Figure 4. Strong current switching is observed for all such devices, with V_{on} values in the range −2 to 4 V, and consistent field-effect mobilities >3 $cm^2\ V^{-1}\ s^{-1}$ (at $40V_{GS}$). I_{on}/I_{off} ratios are ∼10^6, minimal hysteresis is observed, and for the device parameters summarized in Figure 4, S = 1.3 V dec^{-1}.

Spin-coating is a valuable tool for large-area film deposition, but does not offer digital patterning and additive processing capabilities essential for high-speed printing applications. Ink-jet printing was therefore used to deposit ZnO channels for integration into TFTs on thermally grown SiO_2. Because of the

(36) Kajikawa, Y. *J. Cryst. Growth* **2006**, *289*, 387.
(37) Hong, D.; Yerubandi, G.; Chiang, H. Q.; Spiegelberg, M. C.; Wager, J. F. *Crit. Rev. Solid-State Mater.* **2008**, *33*, 101.
(38) Schroder, D. K., *Semiconductor Material and Device Characterization*, 2nd ed.; John Wiley and Sons: New York, 1998.

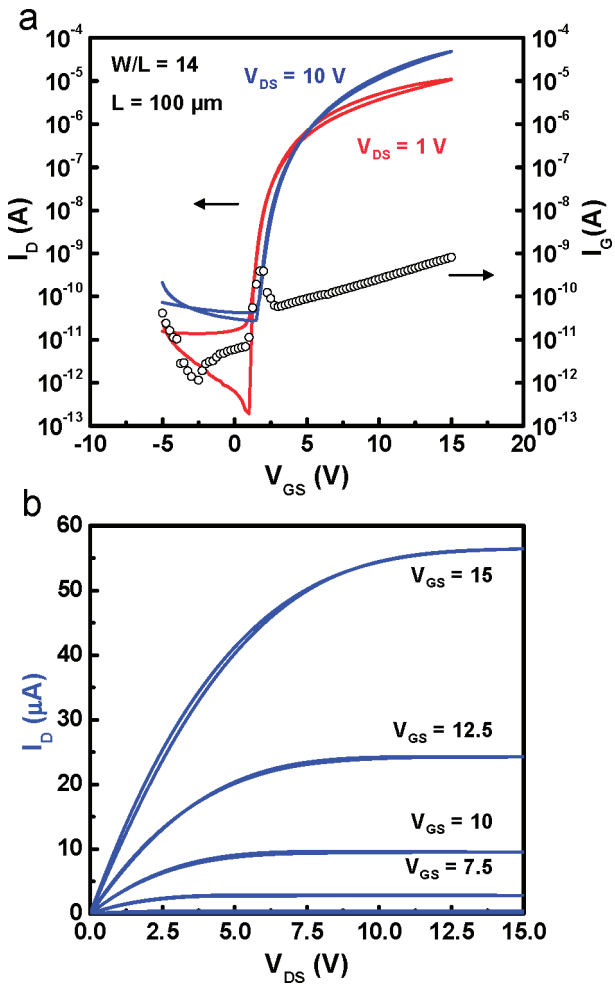

Figure 6. $\log(I_D) - V_{GS}$ transfer characteristics (a) and $I_D - V_{GS}$ output characteristics (b) for a TFT incorporating a 60-nm spin-coated AlPO gate dielectric ($\varepsilon_r = 4.8$) annealed at 500 °C and a spin-coated ZnO-channel annealed at 150 °C in air. $V_{th} = 6$ V.

physical constraints of the available commercial cartridges, isopropanol was added to stock zinc−ammine precursors to decrease solution surface tension and enable reliable jetting. As an undesirable though necessary addition from a chemical standpoint, a high volatility alcohol was chosen to minimize the effect on hydroxide condensation reactions following deposition. No effort was made to test the resolution limits of TIJ printing for individual TFTs, rather printed channels were simple 1 mm × 15 mm stripes intended solely to demonstrate process feasibility.

TFTs fabricated from ink-jet printed ZnO channels annealed in air at 300 °C exhibited inconsistent performance with generally higher V_{on} values, increased hysteresis, and lower mobilities (~2 cm^2 V^{-1} s^{-1}) when compared with spin-coated counterparts. This performance degradation is thought to stem from the requisite use of isopropanol in the printing process, which disrupts condensation and crystallization processes, leading to a higher density of trap states and correspondingly depressed performance.

Because the magnitude of the electrostatic barrier resulting from electron-trapping defects localized at grain boundaries in polycrystalline-channel TFTs scales inversely with carrier concentration[39,40] significant improvements in both mobility and threshold voltage are possible by increasing the carrier concentration. Therefore, by annealing the channel in reducing conditions (analogous to oxygen partial pressure control during vacuum deposition[5]) oxygen vacancies and resultant additional carriers can be produced to improve device performance. Postdeposition annealing of ink-jet printed ZnO channels on SiO_2 for 1 h at 300 °C in flowing inert gas reproducibly generated transistors with field-effect mobilities from 4−6 cm^2 V^{-1} s^{-1} and current−voltage characteristics similar to those in Figure 5a. μ_{inc} for the device shown is 4.3 cm^2 V^{-1} s^{-1} at $40V_{GS}$ and $S = 0.75$ V dec^{-1}, though ~1 V of clockwise hysteresis remains evident. I_{on}/I_{off} is consistently $>10^6$, while hard current saturation at moderate V_{DS} values is apparent in the output curves shown in Figure 5b. These devices offer mobilities comparable to the highest reported for solution processed ZnO TFTs annealed at 500 °C, as well as considerably lower operating voltages (low subthreshold swing), and enhancement-mode operation (i.e., V_{on} is positive).

TIJ-printed ZnO transistors were found to exhibit strong field effect after anneals as low as 100 °C, although nonideal behavior (hysteresis, poor bias stability, and $V_{on} > 20$ V) limited their efficacy. Qualitative TFT operation was achieved after annealing at 150 °C for 2 h in an ambient of flowing N_2; typical transfer and output curves are depicted in Figure 5b. Hard saturation of the output curves is again observed, indicative of efficient pinch-off of the channel. At 12 V, V_{on} is higher than desired for most applications, presumably arising from higher defect (electron trap) densities, which may also be reflected in the ~1.5 V of hysteresis in the transfer curve. μ_{inc} as calculated from the transconductance is 0.41 cm^2 V^{-1} s^{-1} at $40V_{GS}$ for this device. Preliminary bias-stress testing of ZnO-channel TFTs on SiO_2 processed at 150 and 300 °C indicates behavior similar to that reported by Cross and Souza,[41] i.e., a positive shift in V_{th}/V_{on} under a constant positive V_{GS}. However, comprehensive evaluation of bias stability requires development of an appropriate solution-processed passivation layer.[42]

Annealing printed ZnO films in flowing N_2 at temperatures >300 °C produced highly conductive channels, to the extent that after an anneal >400 °C the channel cannot be turned off, even with a $V_{GS} < -20$ V. This is presumably due to the creation of a high density of oxygen vacancies and a concomitant conduction band electron density under nonequilibrium processing conditions. TFTs annealed from 400−500 °C in air are functional, exhibiting increasingly negative turn-on voltages, negligible hysteresis, and hard saturation. Current−voltage characteristics for TFTs annealed at 500 °C in air are comparable to those reported by Ong and co-workers at similar temperatures with V_{on} near −7 V and $\mu_{inc} \approx 6$ cm^2 V^{-1} s^{-1}.[19]

The realization of printed, all-oxide electronics requires the integration of a complete printable oxide materials set, including insulators and semiconductors. To this end, bottom-gate TFTs were fabricated by spin-coating ZnO channels onto solution-processed aluminum oxide phosphate (AlPO) gate dielectric films on p++ Si substrates and evaporating Al source and drain electrodes. Detailed characterization and chemistries for AlPO

(39) Hossain, F. M.; Nishii, J.; Takagi, S.; Ohtomo, A.; Fukumura, T. *J. Appl. Phys.* **2003**, *94*, 7768.
(40) Wager, F. F.; Keszler, D. A.; Presley, R. L. *Transparent Electronics*; Springer: New York, 2008.
(41) Cross, R. B. M.; De Souza, M. M. *Appl. Phys. Lett.* **2006**, *89*, 263513.
(42) Levy, D. H.; Freeman, D.; Nelson, S. F.; Cowdery-Corvan, P. J.; Irving, L. M. *Appl. Phys. Lett.* **2008**, *92*, 192101.

dielectrics have been reported elsewhere.[24] AlPO gate dielectrics were annealed at 500 °C prior to channel deposition; the completed dielectric-semiconductor stack was annealed for 4 h at 150 °C in air following ZnO channel deposition. Representative current−voltage curves for TFTs with 60-nm AlPO gate insulators with a relative dielectric constant of 4.8 are shown in Figure 6. These devices exhibit peak incremental mobilities of ~1.8 $cm^2\ V^{-1}\ s^{-1}$ at $15V_{GS}$, and, notably, gate leakage remains <1 nA. The enhanced gate capacitance density (~2×) of these AlPO dielectrics relative to the 100-nm thermally grown SiO_2 insulators used in the aforementioned devices has a significant impact on device performance. *S* is reduced to 0.36 V dec^{-1} with negligible subthreshold hysteresis, while I_{on}/I_{off} remains $>10^6$ at a $V_{GS} - V_{on}$ value of only 14 V. The excellent performance of these test vehicles notwithstanding, the elimination of the high-temperature anneal required to for the gate dielectric, as well as bias stability analysis (important for all low-temperature oxide TFTs) warrant further study. Nevertheless, we believe this device represents an important milestone in the development of printed oxide electronics, and is to our knowledge the first reported TFT with both solution deposited oxide gate dielectric and channel layer.

The device physics of polycrystalline TFTs are dominated by grain boundary effects; the concentration of deep level defects at grain boundaries and the subsequent formation of depletion regions and double Schottky barriers facilitate both current modulation and a strong bias dependent mobility.[39,43] Because the barrier height (and therefore device mobility) is contingent upon the interplay between carrier concentration and the energy and density of defect states, the effects of different device processing conditions can be difficult to interpret. It is commonly acknowledged that majority-carrier electrons in ZnO arise from oxygen nonstoichiometry, though the precise nature of the contributing defects, whether unintentional impurities, native structures, or surface vacancies is not well established.[44−46] Considering the case of low-temperature deposition of polycrystalline films from aqueous solution, not only is the available thermal energy insufficient to induce the local bond rearrangement and diffusion necessary for minimizing gain boundary defects, but oxygen rich hydroxide intermediates in the present inks naturally result in a film with a low intrinsic carrier concentration following low-temperature curing. The high performance of the devices in the present work may be attributed to the kinetically rapid and thermodynamically favorable low-temperature decomposition to a dense oxide film, which provides a relatively small, though clearly nontrivial defect density. Increasing carrier concentrations above the low intrinsic values through intentional doping (flowing N_2 anneal), or accumulating extra carriers in the channel with higher capacitance gate dielectrics has the demonstrated potential to boost device mobility and functionality.

Conclusion

Exceptional ZnO thin films have been printed from simple and stable precursor inks based on ammine−hydroxo zinc species and integrated into active channel transistors with very limited thermal processing. Incremental device mobilities >5 $cm^2\ V^{-1}\ s^{-1}$ have been achieved with moderate, 300 °C postprocessing, in combination with hard current saturation, enhancement-mode operation, and on-to-off current ratios of 10^6. These represent the highest solution-deposited oxide semiconductor device mobilities reported for any device processed ≤300 °C. Extending the low-temperature precursor chemistry to 150 °C and integration with high-capacitance solution-processed oxide gate dielectrics has allowed printed-channel devices with mobilities of 1.8 $cm^2\ V^{-1}\ s^{-1}$ in tandem with hard current saturation and operating voltages <15 V. These results, coupled with recent demonstration of solution-processed, medium-k Hf based dielectrics[23] demonstrate tremendous potential for the continued development of printed oxide electronics.

Acknowledgment. This work was supported by the Hewlett-Packard Company.

JA808243K

(43) Greve, D. W. *Field Effect Devices and Applications*; Prentice Hall: New York, 1998.
(44) Henrich, V. E.; Cox, P. A. *Surface Science of Metal Oxides*; Cambridge University Press: Cambridge, 1994.
(45) Look, D. C. *J. Electron. Mater.* **2006**, *35*, 1299.
(46) Janotti, A.; Van de Walle, C. G. *J. Cryst. Growth* **2006**, *287*, 58.